Supplementary Information

Scalable Synthesis of [8]Cycloparaphenyleneacetylene Carbon Nanohoop Using Alkyne Metathesis

Xin Zhou,[a] Hyejin Kwon,[b] Richard R. Thompson,[a] Robert J. Herman,[a] Frank R. Fronczek,[a] Carson J. Bruns,[b,c] and Semin Lee[a]*

[a.] Department of Chemistry, Louisiana State University, Baton Rouge, Louisiana 70810, United States

[b.] College of Engineering and Applied Science, University of Colorado Boulder, Boulder, Colorado 80309, United States

[c.] ATLAS Institute, University of Colorado, Boulder, Colorado 80309, United States

Table of Contents

1. General Methods

All commercially available reagents were used without purification. Tris(*tert*-butyl(3,5-dimethylphenyl)amino)(propylidyne)molybdenum(IV) was prepared following reported procedures by Moore and coworkers.[1, 2] Compound **1** was prepared using the methods previously reported.[3-5]

^{1}H NMR (400 MHz and 500 MHz) and ^{13}C NMR (100 MHz and 125 MHz) were recorded on a Bruker AVIII-400 MHz Nanobay or Bruker AVIII 500 MHz at rt (298 K). Chemical shifts (δ) were referenced to tetramethylsilane (TMS) or residual solvent peaks, chloroform (7.26 ppm for ^{1}H NMR, 77.2 ppm for ^{13}C NMR), dichloromethane (5.32 ppm for ^{1}H NMR, 53.84 ppm for ^{13}C NMR). High resolution electrospray ionization (ESI) mass spectrometry was performed on Agilent 6230 TOF LC/MS. Matrix-assisted laser desorption/ionization (MALDI) mass spectrometry was performed on Bruker UltrafleXtreme MALDI. Column chromatography was performed on Biotage Isolera Flash System. Empty flash cartridge housing from Luknova, and Silicycle F60 silica gel (40 – 63 μm, 60 Å) were used for separations. UV-Vis absorption spectra was collected using Agilent Cary 5000 Spectrometer. Fluorescence spectra was collected using PerkinElmer LS 55 Luminescence Spectrometer.

2. Synthesis and Characterization of Compounds

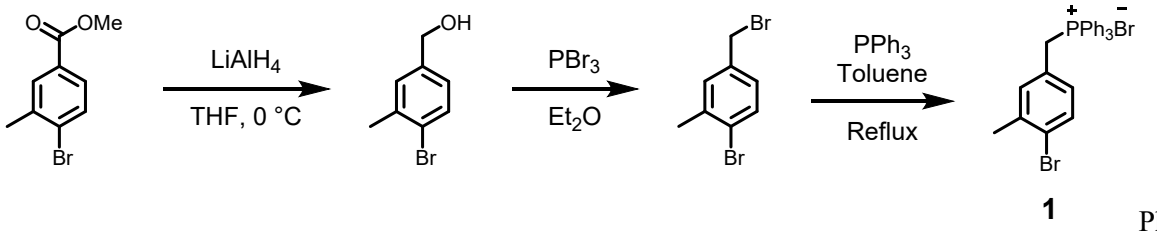

1

Phosphonium salt compound **1** was prepared as reported in the literature.[3-5]

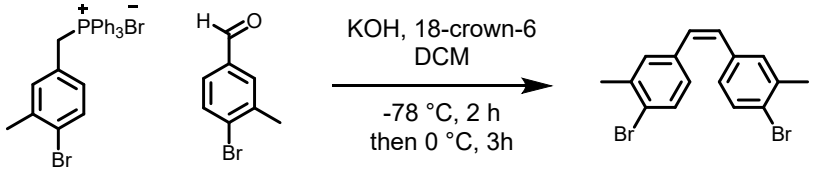

1 **2** **3**

Dibromo-dimethyl stilbene 3 was synthesized following the literature[5]: Compound **1** (10.00 g, 19.00 mmol, 1.0 equiv.), 3-bromo-5-methylbenzaldehyde (3.78 g, 19.0 mmol, 1.0 equiv.) and 18-crown-6 (0.50 g, 1.9 mmol, 0.1 equiv.) were dissolved in DCM (100 ml) at -78 °C. After addition of freshly crushed KOH (2.13 g, 38.0 mmol, 2.0 equiv.), the mixture was stirred at -78 °C for 2 h. Then it was warmed to 0 °C and stirred for 3 h. The reaction was monitored by TLC. After completion, the resulting precipitates were filtered off and washed with hexane. The filtrate was washed with saturated aqueous NH_4Cl solution and dried over Na_2SO_4, filtered, and dried by rotary evaporation. The crude mixture was purified by column chromatography (SiO_2, hexane) yielding the product **3** as white solid (4.23 g, 11.5 mmol, 60%).

^{1}H NMR (400 MHz, $CDCl_3$): δ = 7.36 (d, J = 8 Hz, 2H), 7.12 (d, J = 2 Hz, 2H), 6.91 (dd, J = 8 Hz, 2 Hz, 2H), 6.49 (s, 2H), 2.33 (s, 6H).

^{13}C NMR (100 MHz, CDCl3): δ = 137.95, 136.27, 132.34, 131.41, 129.76, 127.81, 123.80, 22.96.
MALDI-MS: $C_{16}H_{14}Br_2^+$, M^+, calcd. 365.944, found 365.952.

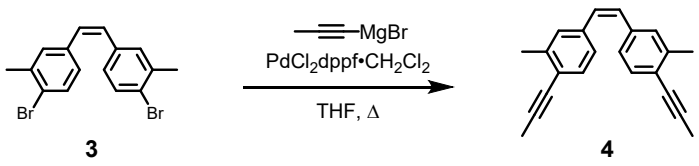

Dipropynyl dimethyl stilbene 4: To a degassed solution of compound **3** (3.00 g, 8.19 mmol, 1.0 equiv.) and $PdCl_2dppf{\cdot}CH_2Cl_2$ (335 mg, 0.41 mmol, 0.05 equiv.) in dry THF (15 ml) was added 1-propynlmagnesium bromide (0.5 M solution in THF, 82 ml, 41.0 mmol, 5.0 equiv.), and heated at 60 °C in a sealed tube overnight. The reaction was cooled to rt and then quenched with water. Most of the THF was removed by rotary evaporation. The mixture was extracted with hexane, dried with $MgSO_4$, filtered, and dried by rotary evaporation. The crude mixture was purified by column chromatography (SiO_2, hexane: DCM 9:1) yielding the product **4** as colorless oil (2.28 g, 8.02 mmol, 98%).

^{1}H NMR (400 MHz, $CDCl_3$): δ = 7.21 (d, J = 8 Hz, 2H), 7.10 (s, 2H), 7.01 (d, J = 8 Hz, 2H), 6.50 (s, 2H), 2.34 (s, 6H), 2.10 (s, 6H).

^{13}C NMR (100 MHz, CDCl3): δ = 139.91, 136.54, 131.75, 130.15, 129.99, 126.10, 122.71, 90.21, 78.85, 20.72, 4.65.

HRMS (ESI-TOF): $C_{22}H_{21}^+$, $[M+H]^+$, calcd. 285.1638, found 285.1630.

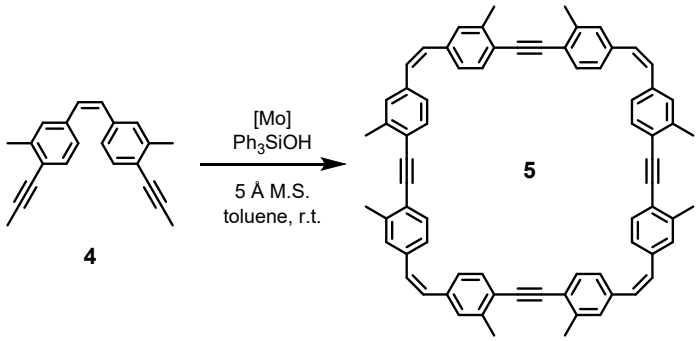

Tetrameric macrocycle 5: Dipropynyl stilbene **4** (1.0 g, 3.52 mmol, 1.0 equiv.), 5 Å molecular sieves powder (4.0 g) was added to dry toluene (100 ml) in a nitrogen-charged glovebox. A solution of tris(*tert*-butyl(3,5-dimethylphenyl)amino)(propylidyne)molybdenum (117 mg, 0.18 mmol, 0.05 equiv.) and Ph_3SiOH (15 mg, 0.5 mmol, 0.15 equiv.) in toluene (10 ml) was stirred in a separate vial for 10 min then added to the reaction mixture. The mixture was stirred at room temperature overnight under nitrogen, then quenched with methanol. Solvent was removed by rotary evaporation. Then the mixture was extracted by Soxhlet extraction with chloroform, and solvent was removed by rotary evaporation. The resulting solid was washed with methanol, and further purified by recrystallization from DCE/Hexane to afford yellow solid (730 mg, 0.79 mmol, 90%).

^{1}H NMR (400 MHz, $CDCl_3$): δ = 7.36 (d, J = 8 Hz, 8H), 7.17 (s, 8H), 7.10 (d, J = 8 Hz, 8H), 6.56 (s, 8H), 2.45 (s, 24H).

^{13}C NMR (100 MHz, CDCl3): δ = 140.06, 137.25, 131.83, 130.41, 130.25, 126.28, 122.30, 93.13, 21.05.

MALDI-MS: $C_{72}H_{56}^+$, M^+, calcd. 920.4382, found 920. 42398.

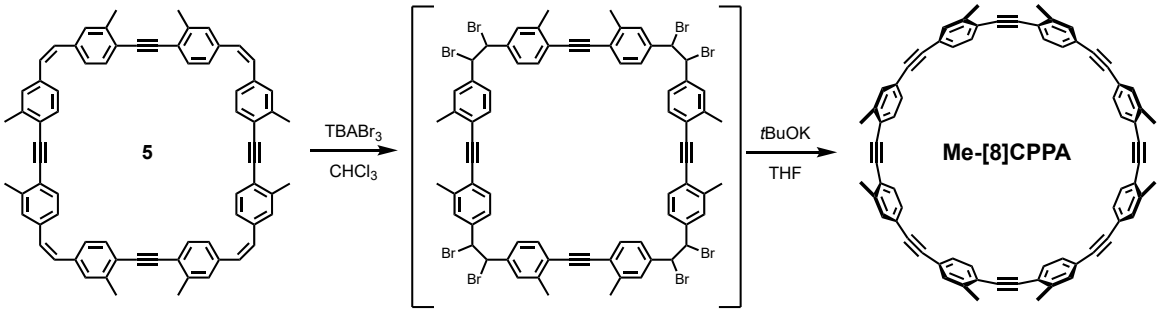

[8]CPPA-Me$_8$: To a solution of tetramer **5** (730 mg, 0.79 mmol, 1.0 equiv.) in $CHCl_3$ (100 ml) was added tetrabutylammonium tribromide ($TBABr_3$) (3.06 g, 6.34 mmol, 8.0 equiv.). The flask was covered with aluminum foil, and the reaction mixture was stirred in the dark for 16 h before quenched with $NaHSO_3$ (aq). The separated organic layer was evaporated. The resulting solid was redissolved in toluene and washed with $NaHCO_3$ (aq) four times times to remove tetrabutylammonium salts. Then the organic layer was dried over $MgSO_4$, and filtered. Solvent was removed by rotary evaporation, and the solid (1.2 g) was subject into the next step without further purification. The brominated macrocycle (1.2 g) was added to dry THF (50 ml) in a nitrogen-charged glovebox. Potassium *tert*-butoxide (KO*t*Bu) (1.38 g, 12.3 mmol, 16 equiv.) was dissolved in dry THF (10 ml). After cooling in the glovebox freezer (–30 °C) for 10 min, the KO*t*Bu/THF solution was added to the macrocycle solution dropwise at rt. The yellow solution turned black during addition, and then stirred at rt for 1 h. The solution was filtered through dry celite and evaporated. Solid was redissolved in toluene and filtered through dry neutral alumina. This step effectively removed the excess KO*t*Bu from the mixture. The solvent was removed to afford desired yellow product **[8]CPPA-Me$_8$** (580 mg, 0.64 mmol, 80% over 2 steps).

^{1}H NMR (500 MHz, $CDCl_3$): δ = 7.39 (d, J = 8 Hz, 8H), 7.32 (s, 8H), 7.25 (d, J = 8 Hz, 8H), 2.46 (s, 24H).

^{13}C NMR (100 MHz, CDCl3): δ = 140.17, 132.41, 132.07, 129.05, 124.33, 123.96, 97.02, 95.08, 20.85.

MALDI-MS: $C_{72}H_{48}^+$, M^+, calcd. 912.3756, found 912.40781.

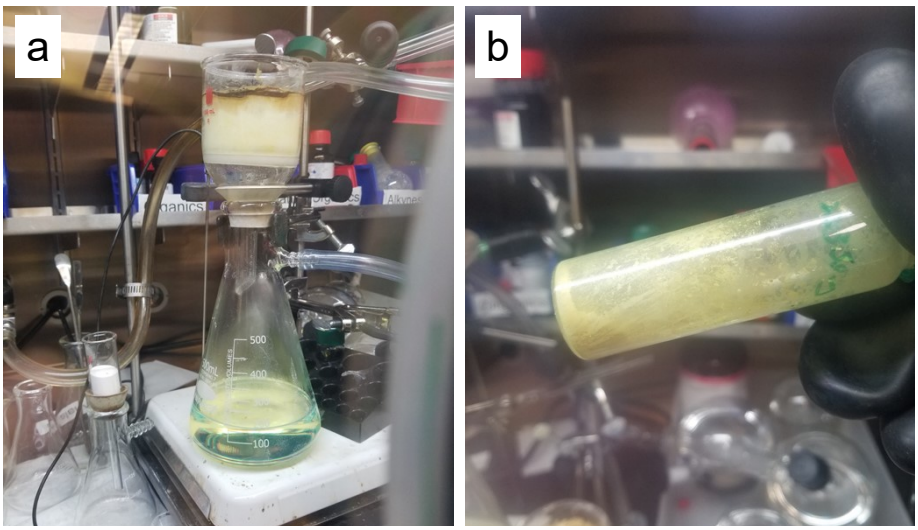

Figure S1. (a) Filtration through a pad of neutral alumina after the dehydrobromination. (b) 580 mg of **[8]CPPA-Me$_8$**.

3. Nuclear Magnetic Resonance Spectra of Compounds

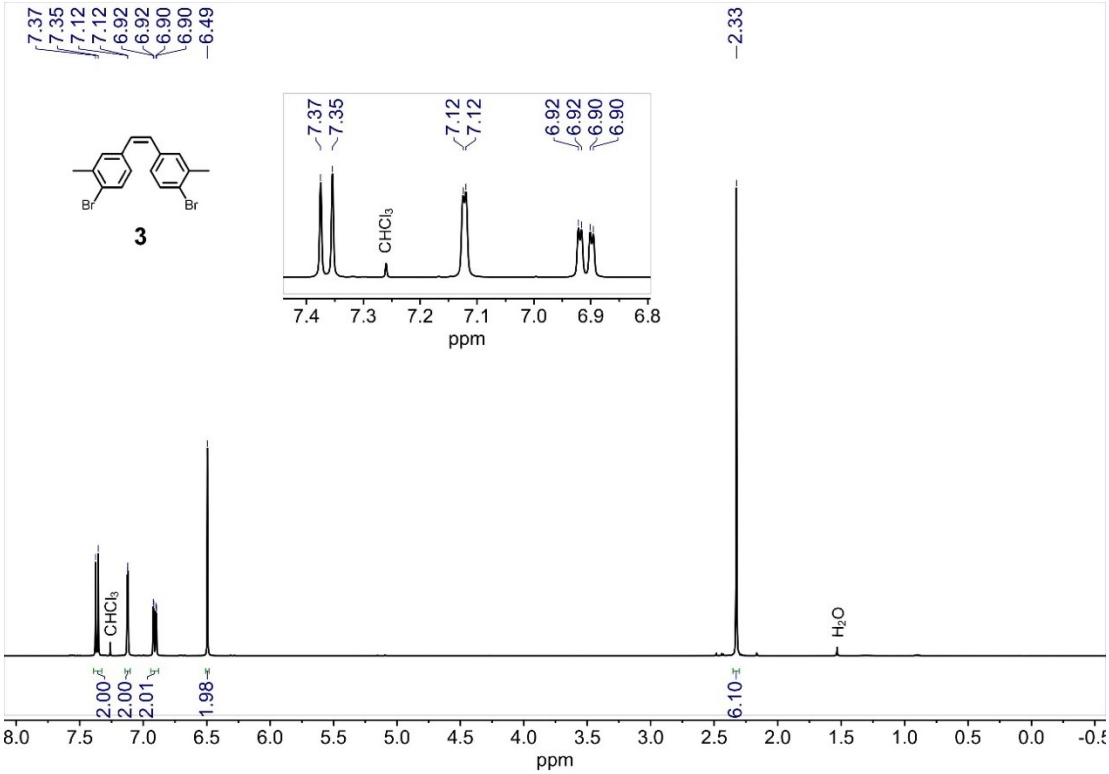

Figure S2. ^{1}H NMR spectrum of **3** (400 MHz, $CDCl_3$).

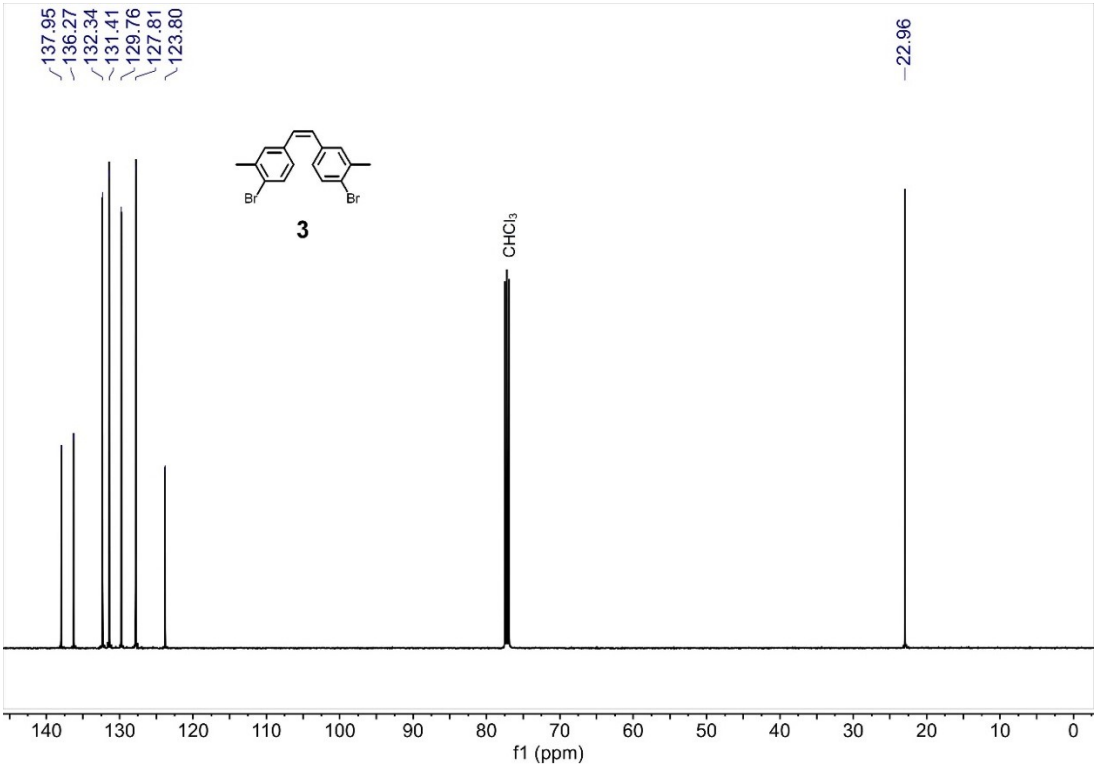

Figure S3. ^{13}C NMR spectrum of **3** (100 MHz, $CDCl_3$).

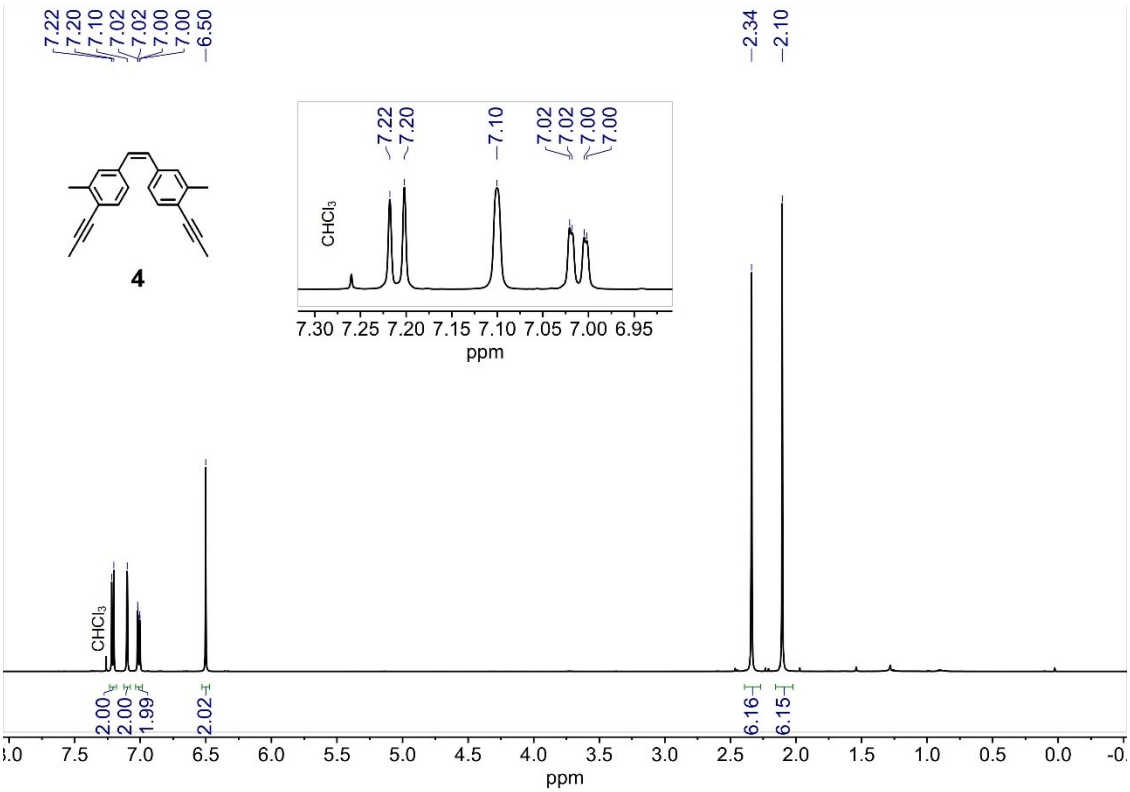

Figure S4. ^{1}H NMR spectrum of **4** (400 MHz, $CDCl_3$).

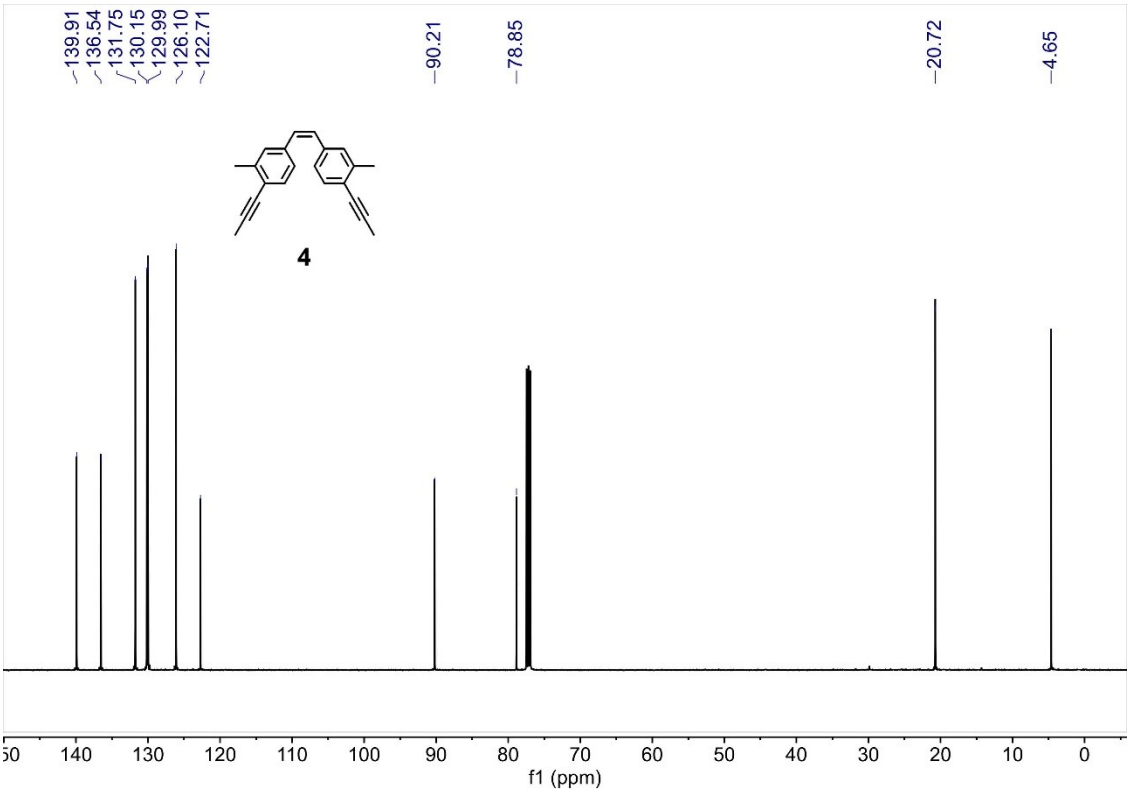

Figure S5. ^{13}C NMR spectrum of **4** (100 MHz, $CDCl_3$).

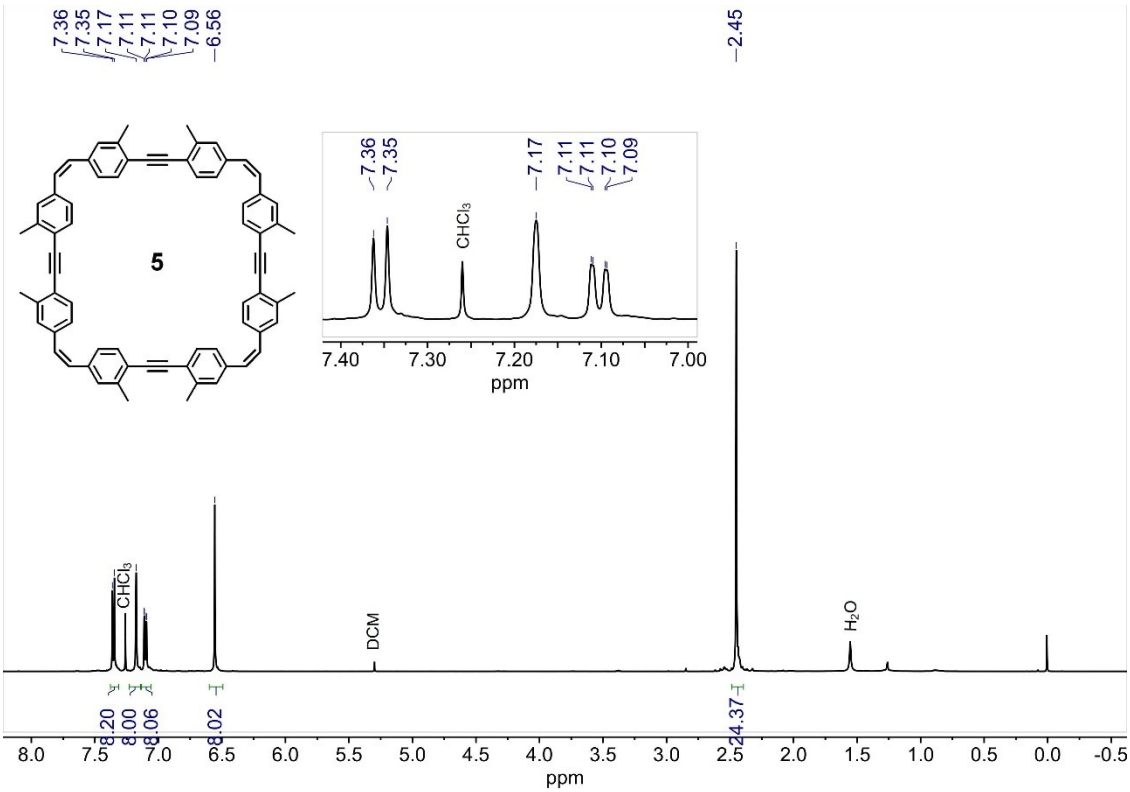

Figure S6. ^{1}H NMR spectrum of **5** (400 MHz, $CDCl_3$).

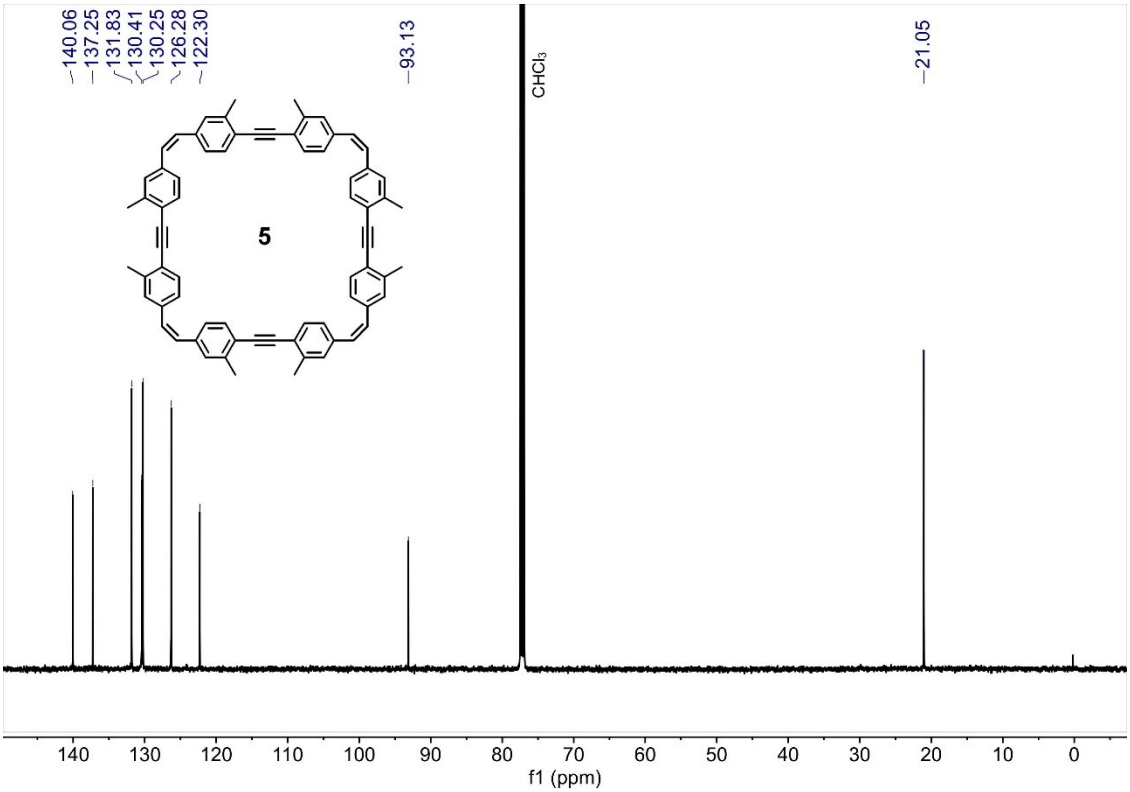

Figure S7. ^{13}C NMR spectrum of **5** (100 MHz, $CDCl_3$).

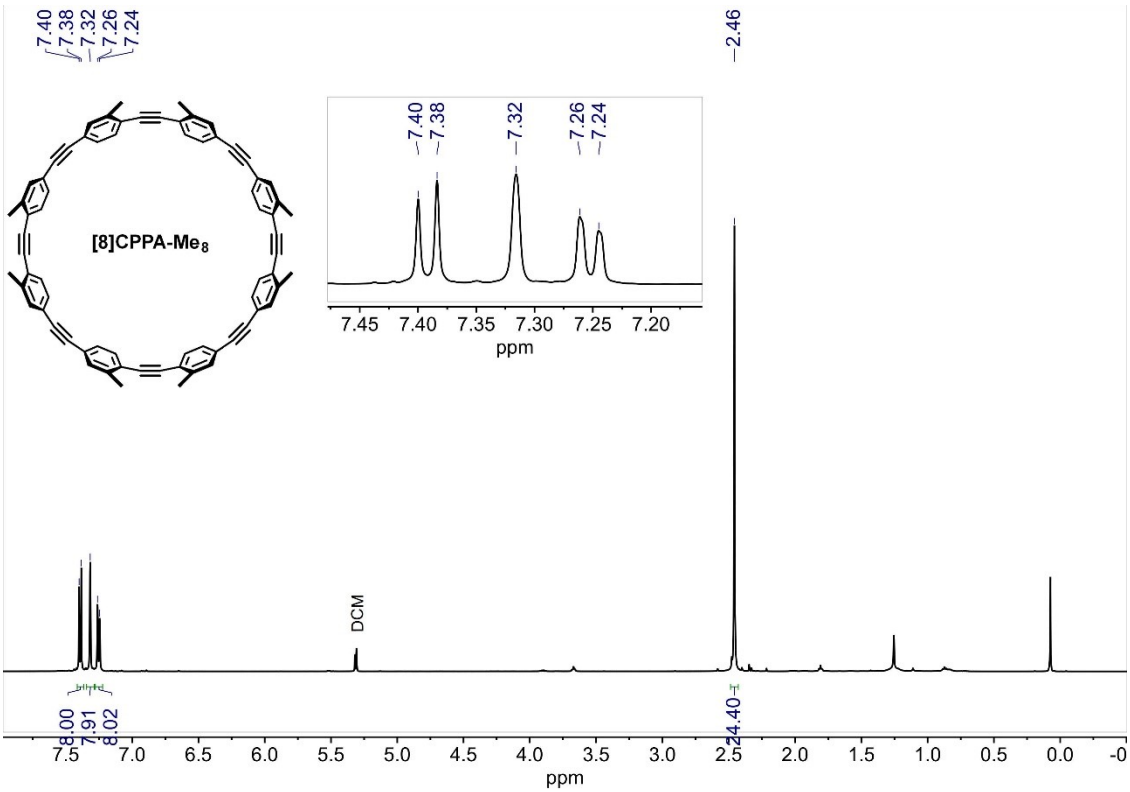

Figure S8. ^{1}H NMR spectrum of **[8]CPPA-Me$_8$** (500 MHz, CD_2Cl_2).

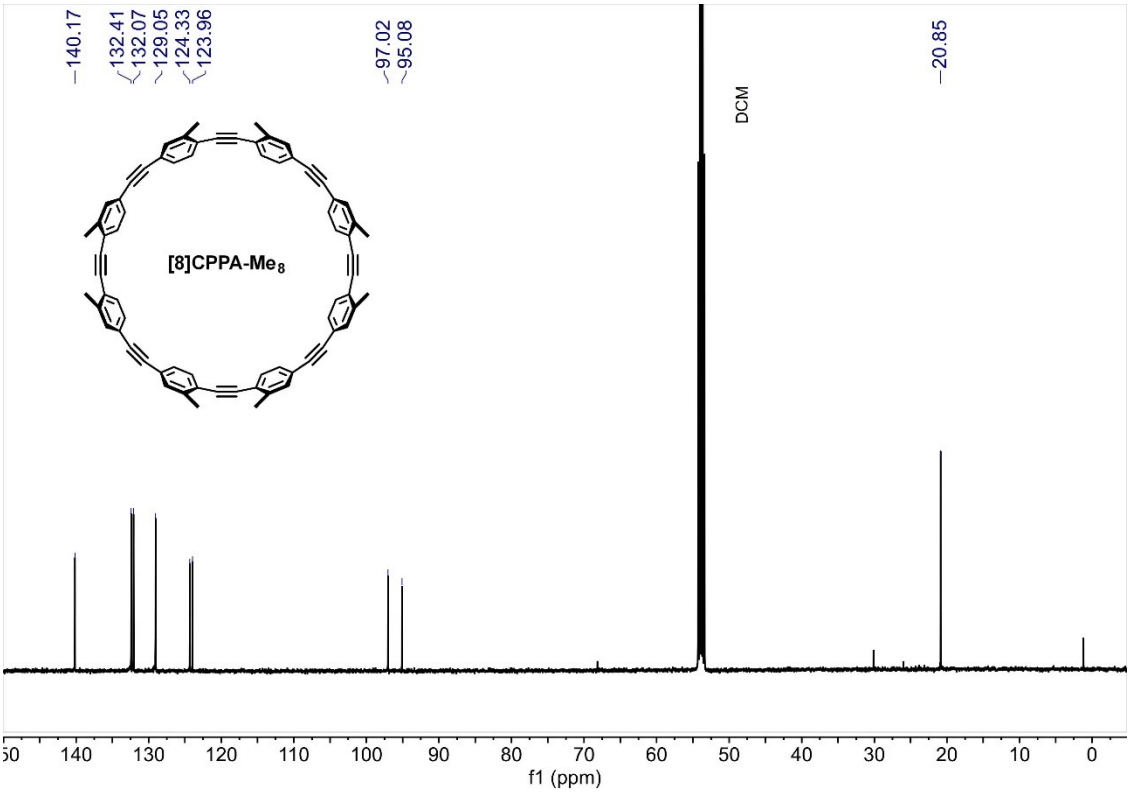

Figure S9. ^{13}C NMR spectrum of **[8]CPPA-Me$_8$** (125 MHz, CD_2Cl_2).

4. UV absorption and fluorescence emission spectra of [8]CPPA-Me_8

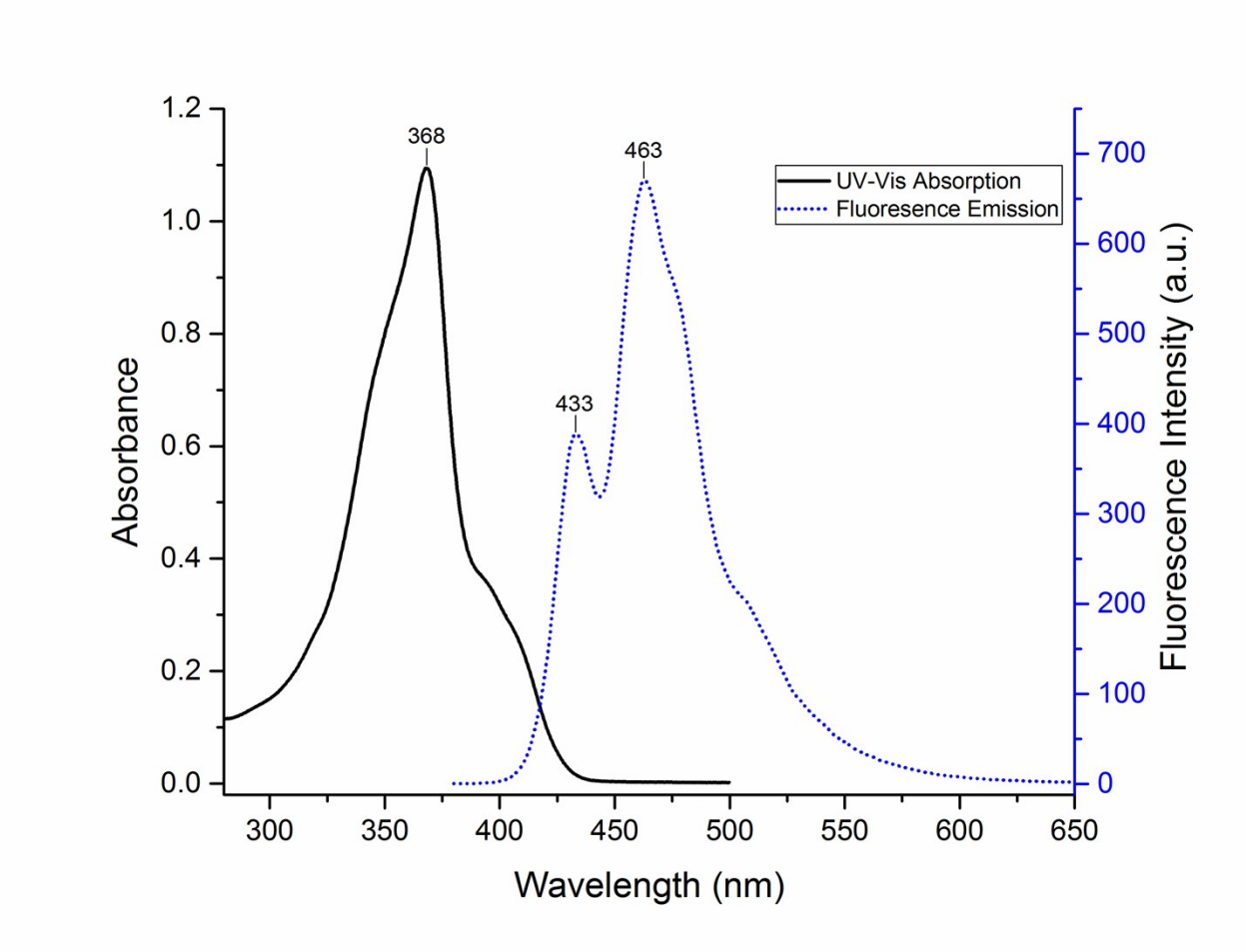

Figure S10. UV-Vis absorption (10 μM, CH_2Cl_2) and emission spectra (10 μM, CH_2Cl_2, λ_{ex} = 368 nm) of **[8]CPPA-Me_8**

5. MALDI Analysis of Alkyne Metathesis products

After the work-up of alkyne metathesis macrocyclization, the crude product (before recrystallization) was subjected into the MALDI analysis. The sample was re-dissolved in 160 µL of dichloromethane (DCM). An aliquot was premixed with matrixes dithranol, in a glass insert before applying 2 µL to the MALDI plate.

Calibration was performed with a standard mixture of peptides to verify intensity and resolution benchmarks. Each spot was irradiated in 40 random locations with 25 laser shots each, resulting in a total of 1000 laser shots. The signal from these 1000 shots was summed to generate a representative spectrum of each spot in the 600-3000 m/z. Ion suppression was used to deflect ions that were not in the mass range monitored. Blank spectra for the matrix solutions were acquired as well.

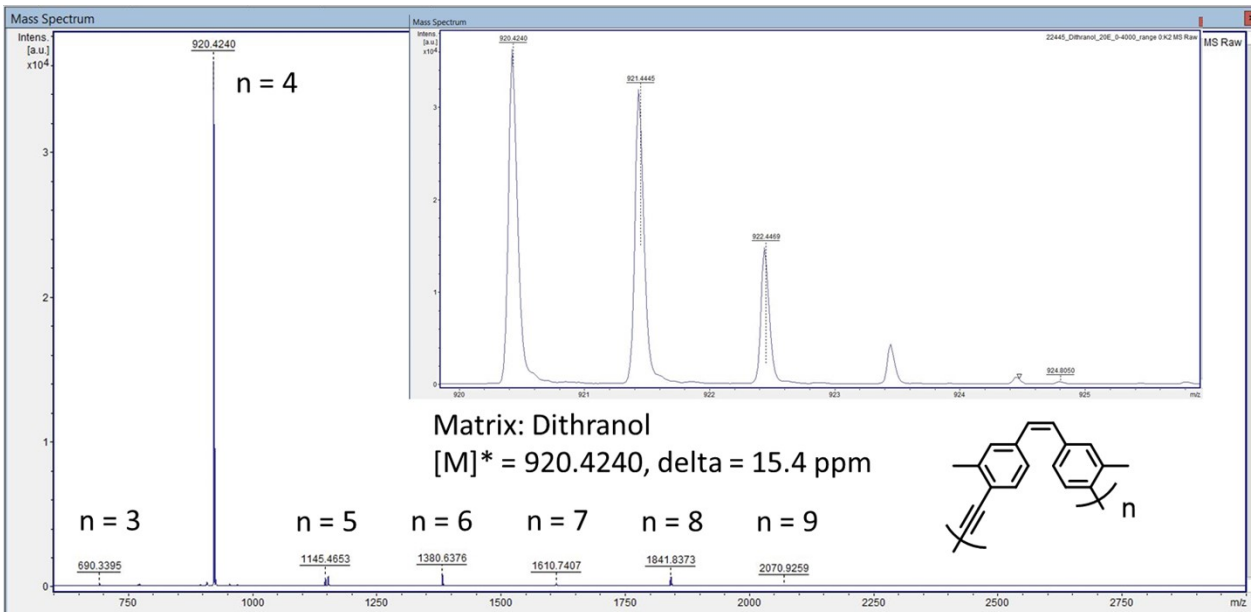

Figure S11. MALDI spectra of the macrocyclic products after alkyne metathesis.

6. X-Ray Crystallographic Analysis of [8]CPPA-Me$_8$

Single crystals of **[8]CPPA-Me$_8$** suitable for X-ray diffraction were prepared by slow diffusion of pentane into a concentrated solution in toluene. The crystal structure was determined using intensity data collected at 90K on a Bruker Apex-II DUO diffractometer with CuKα radiation from a microfocus source. Maximum θ value was 68.0°. Disordered solvent was removed using SQUEEZE, and refinement was vs. the SQUEEZED data. Electrons removed correspond to ca. 10 molecules of toluene per unit cell, or 2.5 per macrocycle. Disordered pentane solvent may also be present. CCDC 2101753.

The molecule lies across a mirror plane in the crystal. Of the four independent methyl groups, all are ordered and on the same face of the molecule, except for one. It exhibits a disorder in which it is on the same face as the others with 43.8(6)% occupancy and on the opposite face with 56.2(6)% occupancy. Thus, the crystal structure is a mix of two isomers (conformers?), with the all-up form being the minor contributor and the form with six methyl groups up and two down being the major contributor.

Crystal data

$C_{72}H_{48}$	D_x = 1.085 Mg m^{-3}
M_r = 1143.43	Cu $K\alpha$ radiation, λ = 1.54184 Å
Orthorhombic, *Pnma*	Cell parameters from 6338 reflections
a = 14.9047 (3) Å	θ = 2.4–68.0°
b = 37.0591 (10) Å	μ = 0.46 mm^{-1}
c = 12.6785 (3) Å	T = 90 K
V = 7003.0 (3) Å^3	Prism, yellow

$Z = 4$	0.20 × 0.17 × 0.12 mm
$F(000) = 2420$	

Data collection

Bruker Kappa APEX-II DUO diffractometer	6525 independent reflections
Radiation source: IμS microfocus	4987 reflections with $I > 2\sigma(I)$
QUAZAR multilayer optics monochromator	$R_{int} = 0.057$
ϕ and ω scans	$\theta_{max} = 68.3°$, $\theta_{min} = 2.4°$
Absorption correction: multi-scan *SADABS* (Krause *et al.*, 2015)	$h = -17 – 15$
$T_{min} = 0.766$, $T_{max} = 0.947$	$k = -44 – 44$
42553 measured reflections	$l = -15 – 14$

Refinement

Refinement on F^2	2 restraints
Least-squares matrix: full	Hydrogen site location: inferred from neighbouring sites
$R[F^2 > 2\sigma(F^2)] = 0.056$	H-atom parameters constrained
$wR(F^2) = 0.160$	$w = 1/[\sigma^2(F_o^2) + (0.0787P)^2 + 2.1715P]$ where $P = (F_o^2 + 2F_c^2)/3$
$S = 1.05$	$(\Delta/\sigma)_{max} < 0.001$
6525 reflections	$\Delta\rho_{max} = 0.27$ e Å^{-3}
340 parameters	$\Delta\rho_{min} = -0.22$ e Å^{-3}

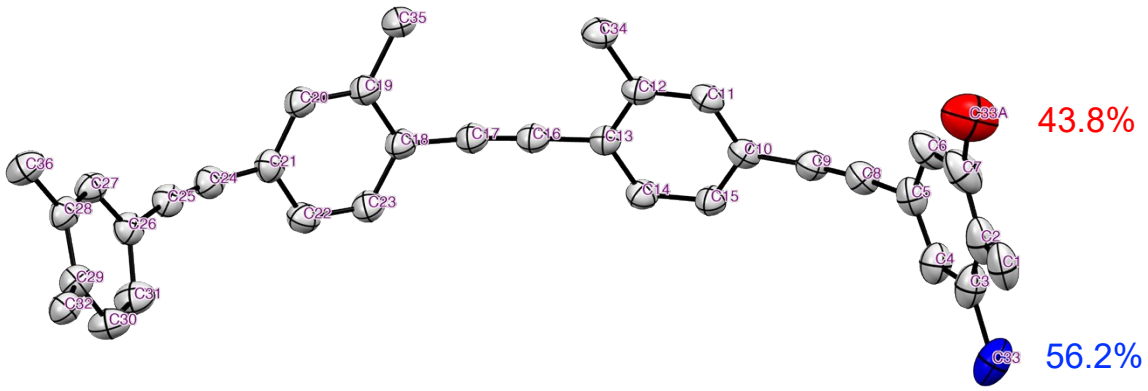

Figure S12. Asymmetric unit of **[8]CPPA-Me$_8$**.

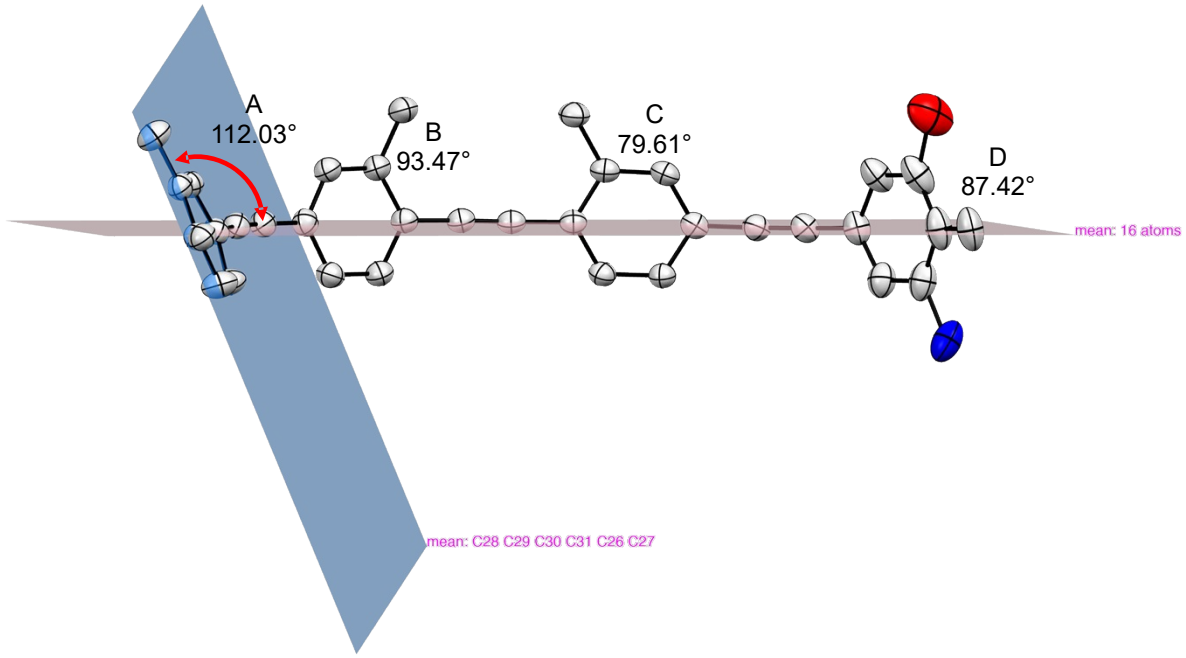

Figure S13. Phenylene angles against the plane of the nanohoop.

7. Computational Analysis of [8]CPPA-Me$_8$ Conformations

With its four di-*o*-tolylacetylene (DTA) units (each adopting either the *Z* or *E* conformation), the **[8]CPP-Me$_8$** ring possesses eight tolyl groups, each representing a plane of chirality. The (*S*,*R*) or (*R*,*S*) configurations of the *Z*-DTA units create local mirror planes of symmetry, leading to four achiral *meso* diastereoisomers of the (*Z*,*Z*,*Z*,*Z*)-[8]CPP-Me$_8$ species. The *E*-DTA units, which may individually possess either the (*S*,*S*) or (*R*,*R*) configuration, may lead to chiral stereoisomers depending on their orientation. There are six (*E*,*E*,*E*,*E*) stereoisomers: two pairs of enantiomers and two *meso* diastereoisomers. Eight chiral species comprising four pairs of enantiomers are present in each of the (*E*,*E*,*E*,*Z*) and (*E*,*Z*,*Z*,*Z*) families of **[8]CPP-Me$_8$** conformers. In the case of the (*E*,*E*,*Z*,*Z*) conformers, there are three pairs of enantiomers when the Me groups of the *Z*-DTA units reside on the same rim, while there is one pair of enantiomers accompanied by two *meso* diastereoisomers when the pairs of *Z*-DTA Me groups are on opposite rims of the macrocycle. Seven (*E*,*Z*,*E*,*Z*) stereoisomers are possible because there are two pairs of enantiomers (one for same-rim and one for opposite-rim orientation of the *Z*-DTA Me groups) and three *meso* isomers (one with same-rim and two with opposite-rim *Z*-DTA Me groups). Therefore, a total of 43 stereoisomers (32 chiral, 11 achiral) can be accessed via 180° rotations of the eight tolyl groups of **[8]CPP-Me$_8$** (***Figure S14***).

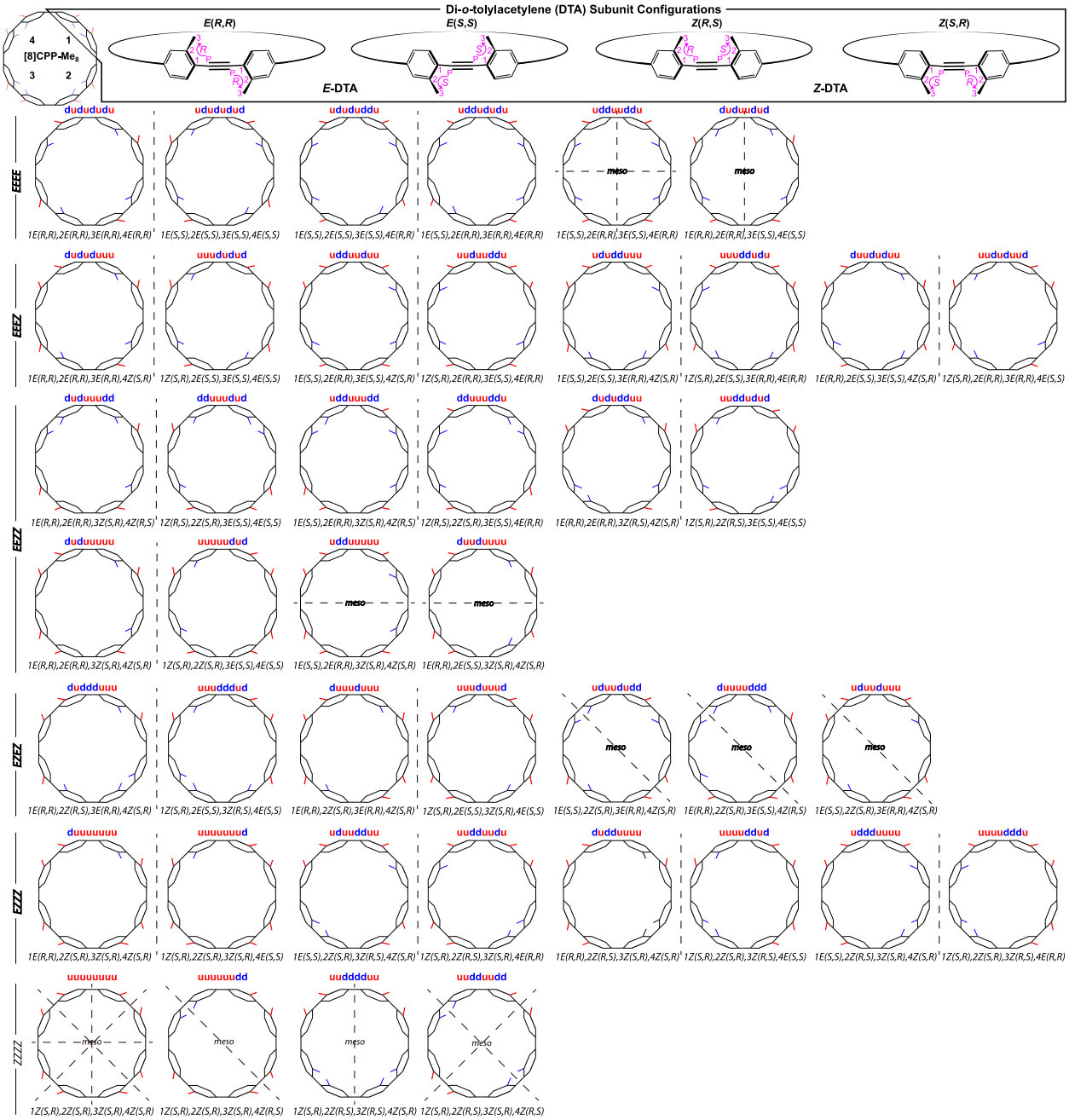

Figure S14. Graphical representations of the 43 possible conformers of **[8]CPPA-Me$_8$**. Dashed lines represent mirror planes of symmetry.

DFT Calculations. We employed Kohn-Sham density functional theory (DFT) to evaluate the relative gas-phase stabilities of the conformers of **[8]CPP-Me$_8$**. DFT calculations were performed with Gaussian16 software using the RMACC Summit Supercomputer, University of Colorado Boulder Research Computing Group.[6] Geometry optimizations of each **[8]CPPA-Me$_8$** conformer were performed with the 6-31G+(d,p) basis set and the B3LYP functional. The Polarizable Continuum Model (PCM) with chloroform was used for solvent correction. Atoms in molecules (AIM) analysis was performed on the energy-minimized structures using Multiwfn, an open-source wavefunction analyzer software package maintained by Tian Lu at Beijing Kein Research Center for Natural Sciences (http://sobereva.com/multiwfn/).[7] AIM theory was applied to investigate the topology of noncovalent bonding interactions within each conformer. The

wavefunctions for the AIM analysis were obtained from checkpoint files using Gaussian16. Electron density (ρ), Laplacian of electron density ($\nabla^2\rho$), and eigenvalues of Hessian (λ_1, λ_2, and λ_3) were computed at intramolecular bond paths with (3,–1) bond critical points (CPs) using Multiwfn software. In AIM analysis, hydrogen-hydrogen bonds were identified at the (3,-1) CPs between hydrogen atoms.

A comparison of 18 conformers of **[8]CPPA-Me$_8$** (***Figure S15***) reveals a clear energetic preference for same-rim orientations of the Me groups. The most stable conformer is the "all-up" [1*Z*-(*S,R*),2*Z*-(*S,R*),3*Z*-(*S,R*),4*Z*-(*S,R*)] conformer (labeled uuuuuuuu for brevity), in which all eight Me groups reside on the same rim of the macrocycle. This conformer's relative stabilization energy (Δ*E*) with respect to the least-stable fully alternating [1*E*-*(RR),*2*E*-*(R,R)*,3*E*-*(R,R),*4*E*-*(R,R)*] conformer (udududud, and presumably its enantiomer dudududu) is –0.142 kcal/mol. When PCM corrections are included ($CHCl_3$), this stabilization is further magnified to –0.240 kcal/mol. The second-most stable enantiomers, possessing seven same-rim Me groups, are [1*E*-*(R,R),*2*Z*-*(S,R)*,3*Z*-*(S,R)*,4*Z*-*(S,R)*] (duuuuuuu, Δ*E* = –0.117 kcal/mol) and presumably its mirror-image conformer uuuuuuud, followed by the *ZZZZ* conformer [1*Z*-*(S,R)*,2*Z*-*(S,R)*,3*Z*-*(S,R)*,4*Z*-*(R,S)*] (uuuuuudd, Δ*E* = –0.110 kcal/mol) with six adjacent Me groups. These lowest-lying gas-phase conformers also dominate the solid-state structure of the **[8]CPP-Me$_8$** macrocycle.

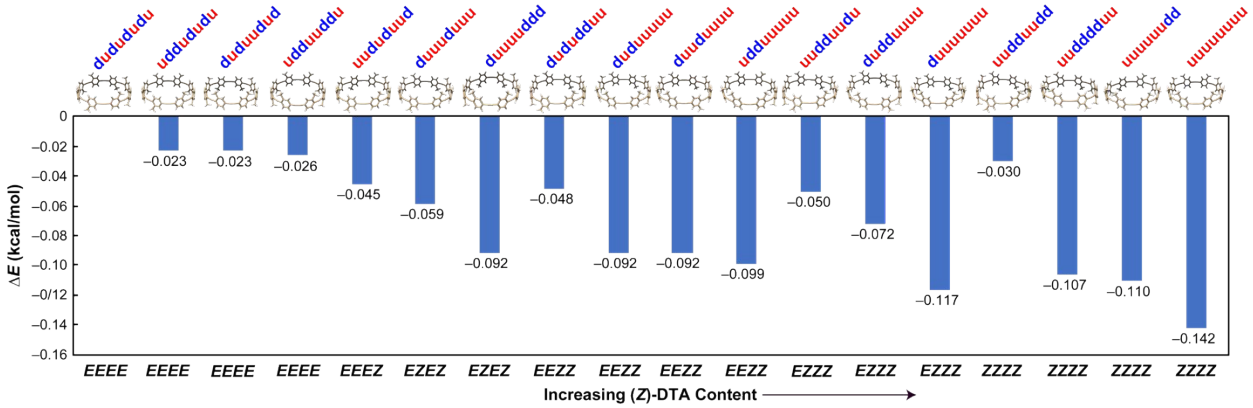

Figure S15. Calculated relative energies of 18 conformers of **[8]CPPA-Me$_8$**.

The (*Z*)-DTA units are more stable than the (*E*)-DTA units, which can be inferred by comparing, for example, the *ZZZZ* conformer [1*Z*-(*S,R*),2*Z*-(*S,R*),3*Z*-(*S,R*),4*Z*-(*R,S*)] (Δ*E* = –0.110 kcal/mol) with the *EEZZ* conformer [1*E*-(*S,S*),2*E*-(*R,R*),3*Z*-(*S,R*),4*Z*-(*S,R*)] (Δ*E* = –0.099 kcal/mol), each possessing six adjacent same-rim Me groups. Likewise, the *ZZZZ* conformer [1*Z*-(*SR*),2*Z*-(*RS*),3*Z*-(*S,R*),4*Z*-(*R,S*)] (Δ*E* = –0.030 kcal/mol) is slightly more stable than the *EEEE* conformer [1*E*-(*S,S*),2*E*-(*R,R*),3*E*-(*S,S*),4*E*-(*R,R*)] (Δ*E* = –0.026 kcal/mol), though each have staggered pairs of same-rim Me groups. The *ZZZZ* conformer [1*Z*-(*S,R*),2*Z*-(*S,R*),3*Z*-(*R,S*),4*Z*-(*R,S*)] (Δ*E* = –0.107 kcal/mol) is also more stable than the *EZEZ* conformer [1*E*-(*R,R*),2*Z*-(*S,R*),3*E*-(*S,S*),4*Z*-(*R,S*)] (Δ*E* = –0.092 kcal/mol) even though both species have two pairs (one on each rim) of four adjacent Me groups. The higher stability of (*Z*)-DTA can be explained by the presence of weak hydrogen-hydrogen bonds [6, 7] between the adjacent methyl groups. AIM analysis revealed the presence of (3,–1) CPs between hydrogen atoms in these (*Z*)-conformers, indicative of intramolecular non-covalent bond paths that are not present in the (*E*)-conformers (see ***Figure 2a*** in the main text). We also observe an energetic incentive for Me groups on adjacent DTA units to occupy the same rim of the macrocycle, explaining why, e.g., the *EZZZ* conformer with seven consecutive same-rim Me groups is more stable than the *ZZZZ* conformer with only six consecutive same-rim Me groups, but the reason for this stabilization effect is not clarified by the AIM analysis.

References

1. W. Zhang, S. Kraft and J. S. Moore, *Chem. Commun.*, 2003, 832-833.
2. W. Zhang, Y. Lu and J. S. Moore, *Org. Synth.*, 2007, **84**, 163.
3. J. P. Olson, M. G. Gichinga, E. Butala, H. A. Navarro, B. P. Gilmour and F. I. Carroll, *Organic & Biomolecular Chemistry*, 2011, **9**, 4276-4286.
4. R. Chahboun, J. M. Botubol-Ares, M. J. Durán-Peña, F. Jiménez, R. Alvarez-Manzaneda and E. Alvarez-Manzaneda, *J. Org. Chem.*, 2021, **86**, 8742-8754.
5. M. Linseis, S. Záliš, M. Zabel and R. F. Winter, *J. Am. Chem. Soc.*, 2012, **134**, 16671-16692.
6. C. F. Matta, J. Hernández-Trujillo, T.-H. Tang and R. F. W. Bader, *Chem. Eur. J.*, 2003, **9**, 1940-1951.
7. M.-L. Y. Riu, G. Bistoni and C. C. Cummins, *J. Phys. Chem. A*, 2021, **125**, 6151-6157.